**NUMERICAL NONLINEAR ANALYSIS OF PALACKÝ BRIDGE****\*Petr Kněž**

Klokner Institute, Czech Technical University in Prague, 166 08 Prague, Czech Republic

Author to whom correspondence should be addressed.

Article Received on 07/11/2021

Article Revised on 27/11/2021

Article Accepted on 17/12/2021

**\*Corresponding Author****Petr Kněž**

Klokner Institute, Czech  
Technical University in  
Prague, 166 08 Prague,  
Czech Republic Author to  
whom correspondence  
should be addressed.

**ABSTRACT**

This paper presents the results of a nonlinear numerical analysis of the Palacký Bridge. It is a historical arch stone masonry bridge. The bridge was built in 1878 and it is a protected monument. It carries traffic over the Vltava River in Prague. The input for the calculation was a detailed survey of the structure, a load test and historical documents from the time of construction. The aim of the assessment was to determine the influence of the diagnosed defects on the behaviour of the structure

and to determine its residual load-bearing capacity. A detailed 3D model of the structure of one arch of the bridge was created for the assessment.

**KEYWORDS:** bridge, stone, arch, masonry, nonlinear analysis.**1. INTRODUCTION**

Palacký Bridge is one of the oldest bridges in Prague. It is a bridge structure for tram and road transport over the Vltava River. Palacký Bridge was built in 1876 - 1878. The bridge was built according to the project of Ing. J. Reiter and arch. B. Münzberger. In 1950 - 51 the whole bridge was widened by building reinforced concrete cantilevers.

The bridge has been serving its purpose for almost 150 years, so it was decided to evaluate its condition in detail. For this purpose, a detailed diagnostic evaluation of the bridge's condition was carried out for the purpose of a detailed non-linear numerical analysis. This included determining the material properties of all parts of the bridge structure. A load test was carried out to validate the numerical model.

The aim of the numerical analysis was to evaluate the findings on the behaviour of the bridge structure. Furthermore, the calculation of its load capacity according to the valid standards was carried out.



**Figure 1: View of the bridge.**



**Figure 2: Stone arch of the bridge in detail.**

### 1.1 Description of the bridge

The bridge consists of a total of 7 arches with different spans. They are made of granite blocks and have a span of  $27.2 + 28.8 + 30.4 + 32.0 + 30.4 + 28.8 + 27.2$  m. The bridge is 229 m long in total. The ratio of rise to span is always 0.154. The load bearing structure has a variable thickness. The thickness of the granite block masonry is approximately 1.2 m at the top and 1.55 m at the base.

On the arched construction of granite blocks there is a brick construction of relief chambers. This consists of a transverse central chamber from which five chambers, each about 1.0 m wide, emerge in the longitudinal direction of the bridge towards the tops of the adjacent arches. The ceiling of the chambers is made of brick arches.

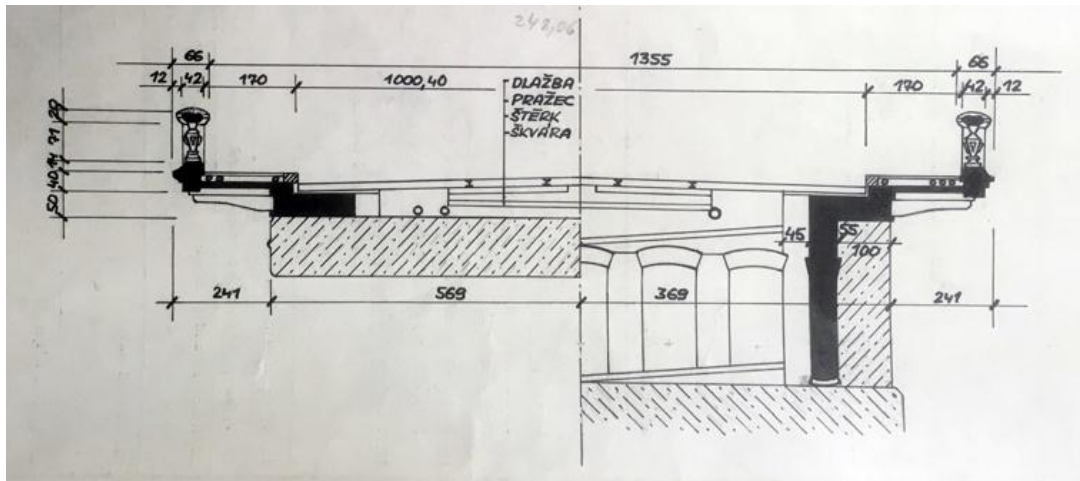


**Figure 3: Cross-section of the bridge (the left half shows the section at the top, the right half shows the section above the pier).**

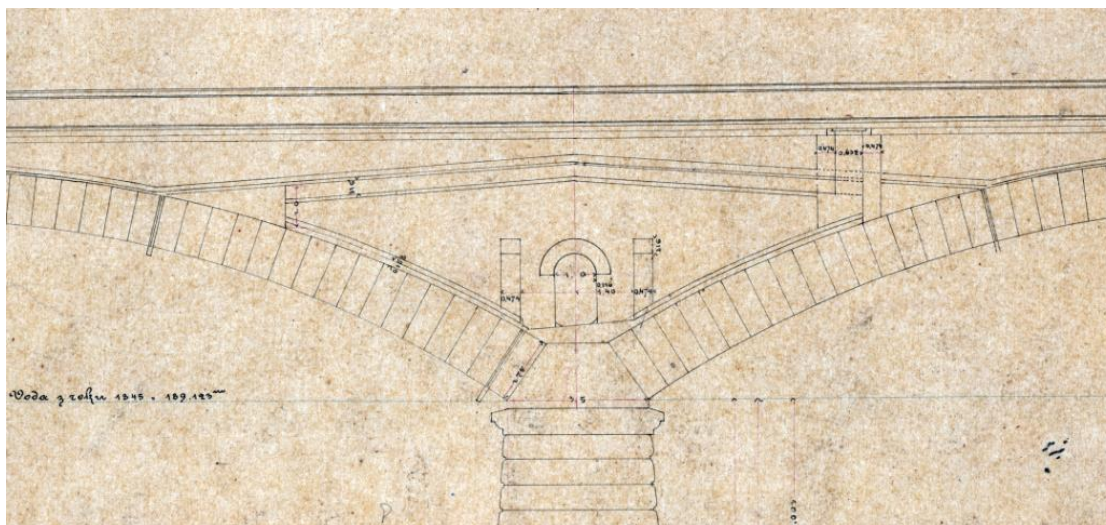


**Figure 4: Longitudinal section through the relief chamber (scan of original drawing from 1875).**

The front walls are made up of several layers. On the view part they are made of sandstone blocks of approx. 0.35 m thick. This is followed by rubble stone masonry, approx. 0.65 m thick. The third layer consists of reinforced concrete, approx. 0.55 m thick, as a vertical continuation of the reinforced concrete brackets. The last layer is the brickwork of the relief chambers.

The pillars are founded on a gravel base. The foundations and the lower part of the pillars are made of concrete, the upper part of granite blocks.

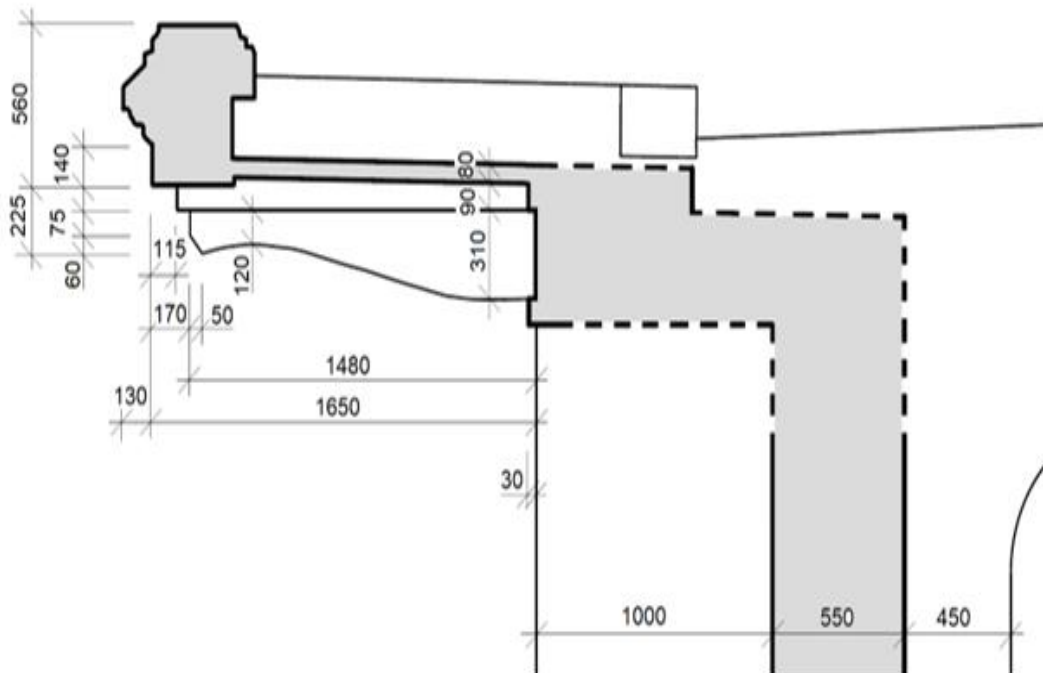


**Figure 5: Cross-section at the location of the widening bridge structure.**

When the bridge was widened in 1950-1951, the width was changed from the original 10.7 m to 13.90 m. The widening is made with variable height cantilever ribs with a span of 1.76 m and a width of 0.24 m. These cantilever ribs have an axial distance of 1.0 m between each other. A reinforced concrete slab with a thickness of 80 mm is placed between the cantilevers. The cantilevers are woven into a massive longitudinal beam placed on the front wall. These beams are continuous throughout the length of the bridge and are made of reinforced concrete. In the areas above the piers and in approximately 1/3 of the span of the arch, the beams are anchored into the massive longitudinal wall created by concreting the edge relief corridor. In the apex of the arch the longitudinal beams lie on the front walls and are probably not anchored into the arch. In order to ensure sufficient stability of the beams in the top parts of the arches, massive transverse stiffening beams of 1.50 m width were made in about 1/3 of the span connecting the beams on the front walls on the left and right sides of the bridge.





**Figure 6: View of the bridge widening.**



**Figure 7: View into the relief chamber.**

## **1.2 Conclusions of the diagnostic survey**

As part of the diagnostic survey, a detailed geodetic survey of the bridge dimensions was carried out and the conformity with the preserved drawing documentation was verified. Another focus of the survey was to evaluate the structural condition of the structure and to

determine the material properties of the structure. The material properties were determined on samples taken from the bridge. These were evaluated by tests in the laboratory. The material properties obtained are presented in the Materials and Methods chapter.

The survey of the condition of the granite block arched structure did not reveal any visible defects that could be caused by static stresses or overloading of the structure. The surface of the granite blocks was slightly degraded in places to a depth of 5 mm. Due to poorly functioning waterproofing of the bridge and seepage, leaching of the binder from the joints was occurring. In about 50% of the locations addressed by the diagnostic survey, poor joint filling with mortar was found on the lower surface of the masonry arches. Mortar was missing in the joints to a depth of 50 - 200 mm. Given the thickness of the vault, this finding does not have a significant effect on the functionality of the masonry of the arches. The granite blocks have roughly worked bearing surfaces and the joint widths are small, so it can be concluded that it was technically very difficult and in some cases impracticable to fill the joints perfectly to the full thickness of the structure when the bridge was built. In our judgment, the observed state of filling the joints with mortar primarily dates back to the construction of the bridge.

The survey of the relief chamber structures did not reveal any visible defects caused by static stresses or overloading. The brickwork of all the relief chambers is plastered. It cannot be ruled out that there are areas of locally degraded masonry under the plaster. Local cracks up to 0.8 mm wide were found in the tops of some of the vaults of the chambers. The condition of the masonry of the relief chambers can be assessed as satisfactory. Water is leaking into the relief chambers.

The survey of the bridge foundation showed that the piers are made of granite masonry blocks up to 1.5 - 2.0 m below the water level. Below the granite blockwork, concrete follows. The parts of the piers above the water level do not show any visible defects caused by static stresses or overloading. The masonry joints are generally well filled with mortar.

No cracks or other static disturbances were found in the front walls. In particular, the sandstone of the outer face layer is damaged and degraded, but it does not play a significant structural role. The degradation is mainly caused by natural erosion of the stone together with frost action.

The greatest damage was found on the widening reinforced concrete structure. In this case, the poorly functioning waterproofing at the expansion joints leads to leakage and subsequent corrosion of the reinforcement. The areas with the worst corrosion damage were assessed as irreparable and recommended for local replacement with new construction.

The diagnostic survey also addressed the installation of long-term temperature measurements in the structure. This was supplemented by geodetic measurements of bridge movements during different seasons. The conclusion of these measurements was that temperature changes induce significantly higher deformation of the structure than the load from traffic on the bridge.

## 2. MATERIALS AND METHODS

This chapter will describe the materials used and their properties obtained from the diagnostic survey. The selected computer software, the material models used and the numerical analysis procedure will be described.

### 2.1 Materials

Based on the tests performed on the materials taken from the bridge structure, the material characteristics of the structure were determined. The values found are given in the following tables 1-4.

**Table 1: Material characteristic of masonry elements according to ČSN EN 772-1+A1.<sup>[1]</sup>**

Type of masonry	Compressive strength $f_c$ [MPa]	Modulus of elasticity $E_b$ [GPa]	Volumetric weight [kg/m <sup>3</sup> ]
Granite	120	44	2700
Bricks	25	not measured	1800
Sandstone	25	14	2000

**Table 2: Material characteristic of mortar according to ČSN EN 998-2.<sup>[2]</sup>**

Type of masonry	Compressive strength $f_m$ [MPa]	Volumetric weight [kg/m <sup>3</sup> ]
Granite	10	1700
Bricks	7	1730
Sandstone	1	1730

**Table 3: Strength and classification of concrete according to ČSN EN 13791.<sup>[3]</sup>**

Occurrence	Compressive strength $f_c$ [MPa]	Strength class
pillar foundations	22,1	C12/15
widening structures	37,9	C25/30

**Table 4: Strength of steel reinforcement according to ČSN 730038.<sup>[4]</sup>**

Type	Yield strength $f_y$ [MPa]	Ultimate strength $f_u$ [MPa]
10 512 Roxor	400	500

## 2.2 Methods

The bridge arch with the largest span (32 m) was selected for analysis. An assessment of the whole bridge would be too demanding for a detailed non-linear analysis. The main load-bearing arch structure of the bridge made of granite stones will be modelled with detailed masonry bond and the imperfect joint filling with mortar will be taken into account. The imperfect mortar joint filling will be addressed by omitting the mortar in the central part of the section for simplicity. The calculation will be carried out in accordance with the standard regulations.<sup>[5,6,7,8,9,10]</sup>

### 2.2.1 Description of the software and material models used

The software Atena 3D,<sup>[11,12,13]</sup> developed by the Czech company Cervenka consulting, was chosen for the nonlinear numerical analysis. It is a specialized program for the assessment of concrete and similar materials, which can include mortar, brick and natural stone. The program allows to define contact tasks and reinforcement of elements with reinforcing bars.

The following material models were chosen for the numerical analysis

- 3D Nonlinear Cementitious 2.<sup>[11,12,13]</sup> has been used to model stone, brick, mortar and concrete. The fracture-plastic model combines constitutive models for tensile (fracture) and compressive (plastic) behavior. The fracture model is based on the classical orthotropic formulation of the smeared crack and the crack band model. It uses Rankine's failure criterion, exponential softening and can be used as a rotated or fixed crack model. The hardening/softening plasticity model is based on the Menétrey-Willam failure surface.
- The Reinforcement material model was used for steel reinforcing bars in concrete elements. The material model is using a conventional bilinear relationship for plasticity based on the yield strength criterion.<sup>[14]</sup>
- The 3D Drucker Prager Plasticity.<sup>[11]</sup> was used to model the embankment. Drucker-Prager plasticity model is based on a general plasticity formulation.



### 2.2.2 Method of model validation

After the geometry of the model was completed, the material properties were validated by comparing the results obtained on the model with those from a static load test performed on the actual structure. For this purpose, the model was loaded with identical loads and the deflection at the measured points from the applied load was compared. The model must also account for the effect of self-weight, but the actual measurements only consider the load increase from the overload of the structure. Therefore, within the model it is necessary to subtract from the results the deformation induced by the dead weight.

## 3. Non-linear analysis of the structure

### 3.1 Description of the created model

The computer model processed in Atena 3D shows the construction of the longest arch of the Palacký Bridge. The static action of the structure is quite complicated. It is strongly influenced by the relief chamber and the bridge widening. All these elements form a series of longitudinal walls on the bridge, which increase the stiffness of the whole structure and help to redistribute the load.

The model was created on the basis of a 3D scan, supplemented by fragments of the original documentation and the conclusions of the diagnostic survey. The model consists of a main stone vault, a brick relief chamber and an expanding reinforced concrete structure. The pillars are modelled with simplified geometry. The model also includes the embankment and the roadway and pavement layers. The total number of macro elements in the model is 5323.

The main stone vault in the model is "bricked" - it consists of individual granite stones with mortar between them. Only 2/3 of the volume of each joint is filled with mortar at all joints - the middle third is without mortar. The granite stones are also divided into thirds along the height for the sake of contact formation. The thickness of the contact joints in the longitudinal direction is variable - 10 mm on the face of the vault and 25 mm on the reverse. The contact joints in the transverse direction have a constant width of 10 mm. Due to the complexity of the model, it was not possible to make the model to the tops of the adjacent arches, so it terminates 5.2 metres behind the axis of the piers. For the widening structure, reinforcement was inserted only in the beams that carry out the pavement slab.

The other masonry structures - the relief chamber, the pillar and the front walls are modelled as homogeneous material with a compressive strength corresponding to the recommendations

of the diagnostic conclusions, a tensile strength of the mortar and a modulus of elasticity determined according to the coefficient  $k = 1000$  (the modulus of elasticity of the masonry can be considered as  $k$  times the characteristic strength of the masonry). The modulus of elasticity was then further adjusted during the validation of the model.

The contacts between the elements are designed as fixed except for the expansion joints of the widening structure. The transformation capacity of the main vault is ensured by mortar-filled joints, which may crack if their strength is exceeded. The total number of contacts in the model is 16867.

The finite element mesh was chosen individually for different types of macro elements to ensure optimal mesh connectivity while keeping the number of finite elements as low as possible. As a result, the mesh has 688993 finite elements.

The bridge support is designed as a fixed support at the bottom surface of the piers. These supports are supplemented by continuity conditions at the points where the structure has been split - displacement in the longitudinal direction is prevented, deformation in the transverse and vertical direction is allowed.

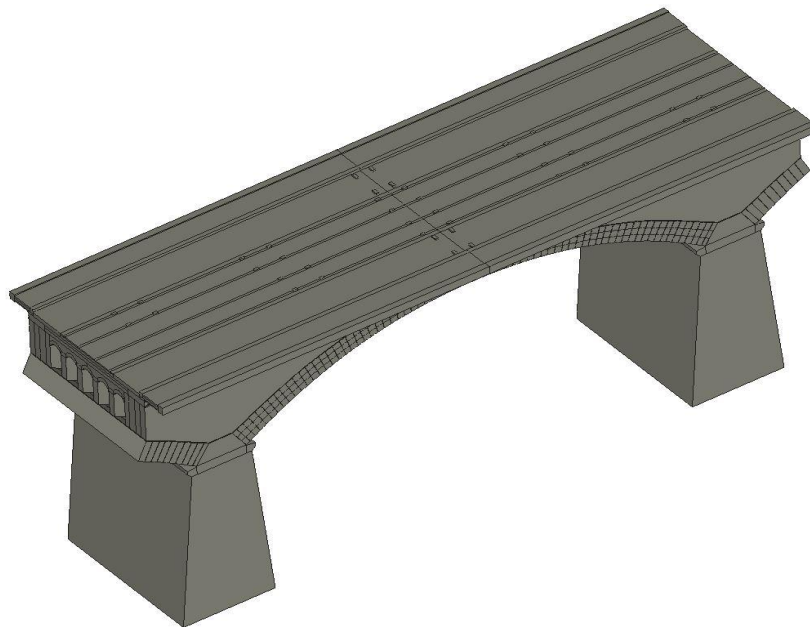


**Figure 8. Created model of the bridge.**

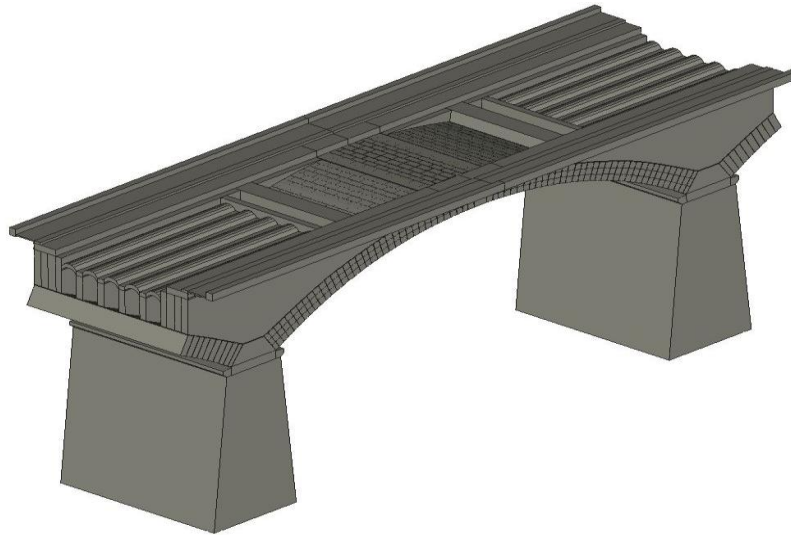


**Figure 9: Created model of the bridge - load-bearing structure only.**

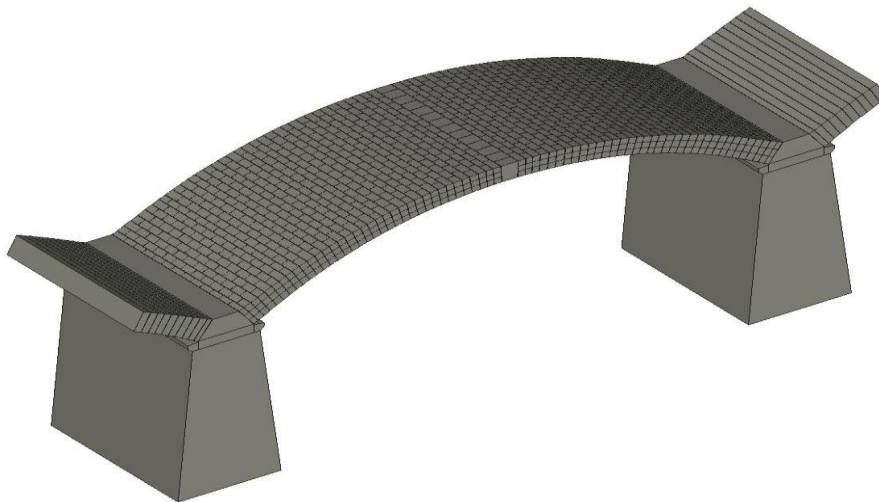


**Figure 10: Created model of the bridge - stone arch only.**

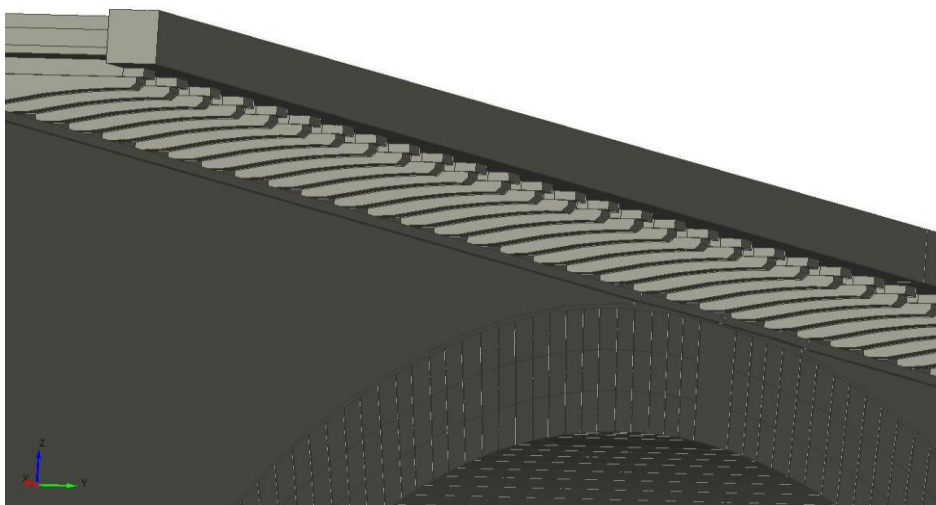


**Figure 11: Detailed view of the extension in place of the pavement.**

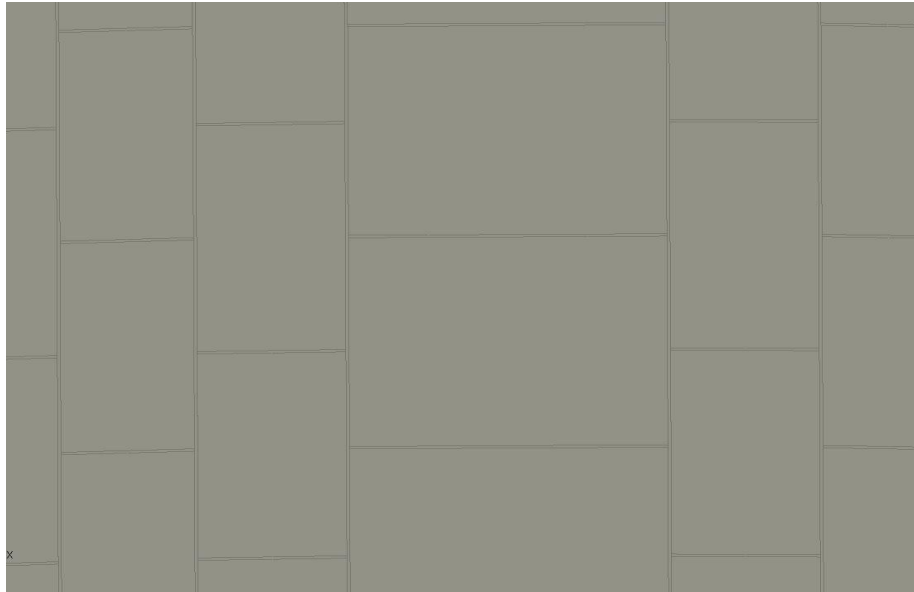


**Figure 12: Detail of the masonry bond of the stone vault in the model.**

### 3.2 Loads considered in the analysis

The model was loaded in accordance with ČSN 73 6222.<sup>[9]</sup> to determine the normal load capacity of the bridge structure. The load was therefore made up of the dead weight of the structure, which was automatically generated by the program based on the specified geometry and the volumetric weight of the individual materials. This load was supplemented by loads representing traffic on the bridge - these were tram sets (the loading scheme is shown in Figure 13), vehicle loads in the lanes and pedestrian loads on the pavements (5 kN/m<sup>2</sup>). The loads from the vehicles consist of the loading vehicle (Figure 14) and the area load. The vehicle has a total mass of 32t (320 kN) and the area load is 9 kN/m<sup>2</sup>. All moving loads were increased by a dynamic factor of 1.05.

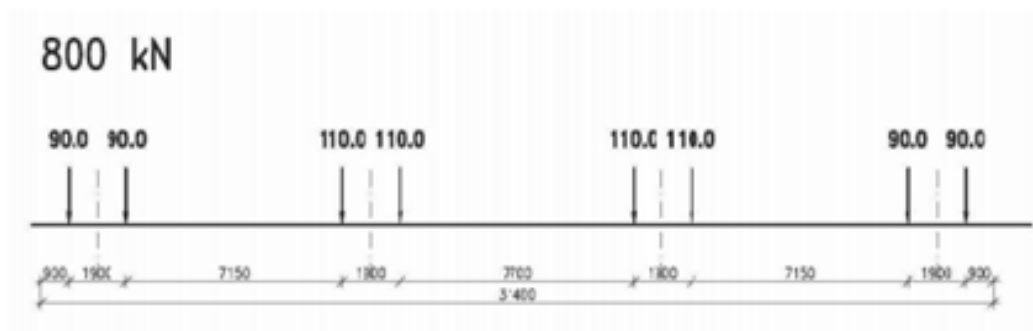


**Figure 13: Load scheme of a tramway vehicle type 15T.<sup>[6]</sup>**



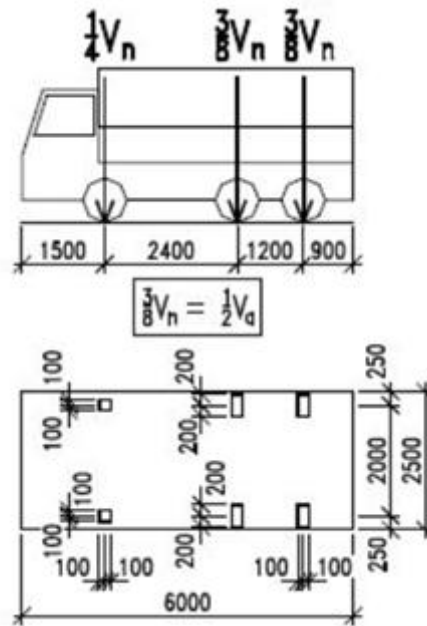


**Figure 14: Load scheme of the transport vehicle.<sup>[9]</sup>**

The model was further loaded with temperature.<sup>[6,10]</sup> The bridge was heated at  $\Delta t + 30^\circ\text{C}$  for warming and  $\Delta t - 30^\circ\text{C}$  for cooling (cooling was the more unfavourable condition and results for this loading will be presented).

In general, the results of the Palacký Bridge temperature measurements show that the internal structure reacts gradually to temperature changes and there is also a noticeable phase shift of this reaction. The structure responds to temperature changes in a delayed manner and does not reflect the step changes in temperature of the external environment.

## 4. RESULTS OF NUMERICAL ANALYSIS

### 4.1 Model validation results

The computational model was validated against the load test results. Due to the larger deformations, a load condition of 3+3 vehicles in the middle of the bridge span (6\*32t) was chosen for validation. The wheels of these vehicles were inserted into the model and loaded with the corresponding forces.

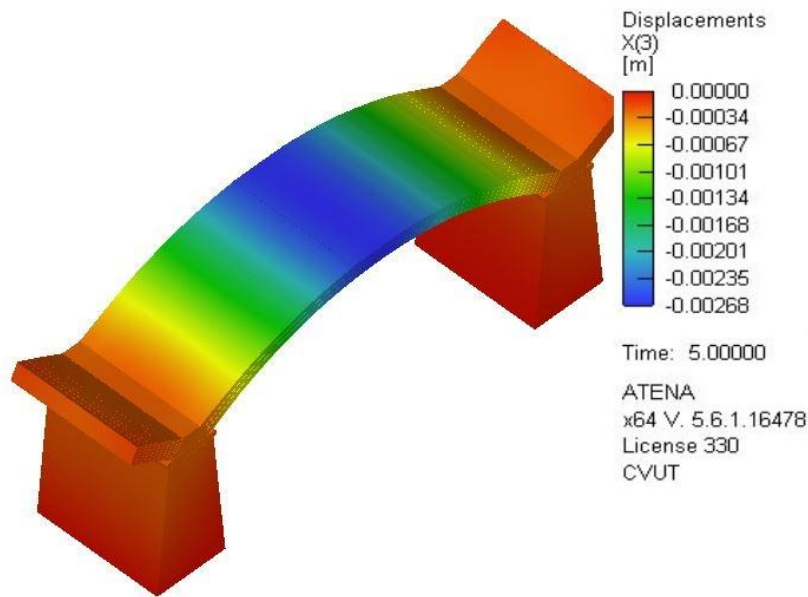


**Figure 15: Deflection from dead weight - 2.68 mm.**

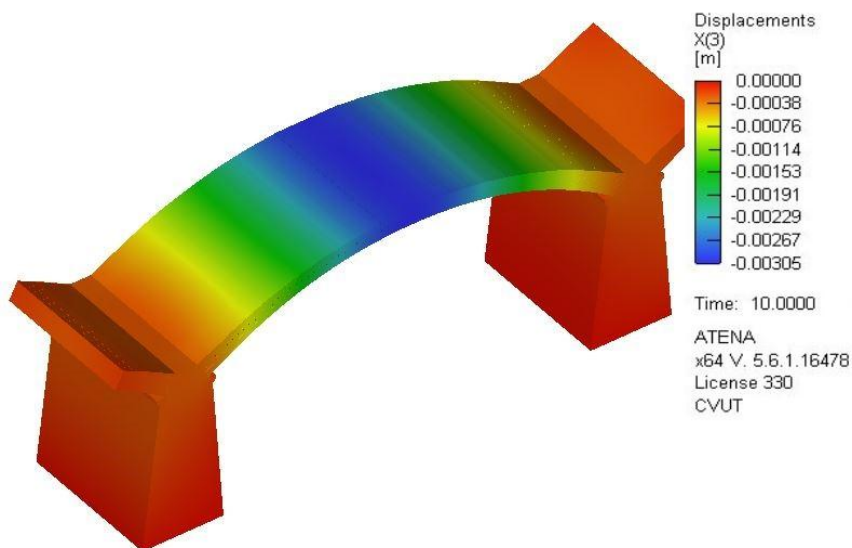


**Figure 16: Deflection from dead weight + load from test load - 3.05 mm.**

From the above figures (15,16) it is possible to read the value of the increase in deformation when the model is loaded with cars. The resulting deflection from this load is  $3.05 - 2.68 = 0.37$  mm. The average deflection for the static load test is 0.43 mm. The difference between the model and the test is therefore 14 %. Due to the very small deflection from the test load, it is difficult to obtain an exact match on the model. A difference of 0.06 mm is an acceptable error.

The load capacity calculation was determined for loads located at the top of the vault. Due to the significant stiffening of the vault in the heel region, up to about one-third of the span of the longitudinal walls, loading the vault in its quarter would not have a significant effect.

#### 4.2 Results for traffic loads

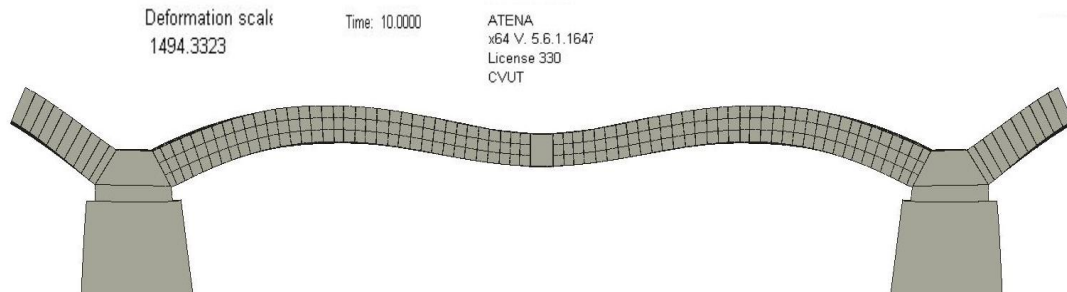


Figure 17: Deformed shape of the structure in 1494:1 scale.

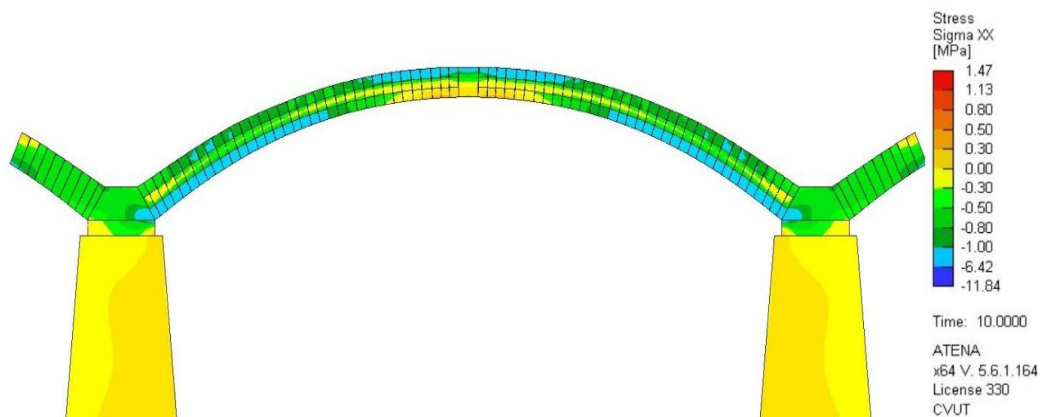


Figure 18: Stress in the longitudinal direction in the vault section - maximum 1.47 MPa, minimum -11.84 MPa.

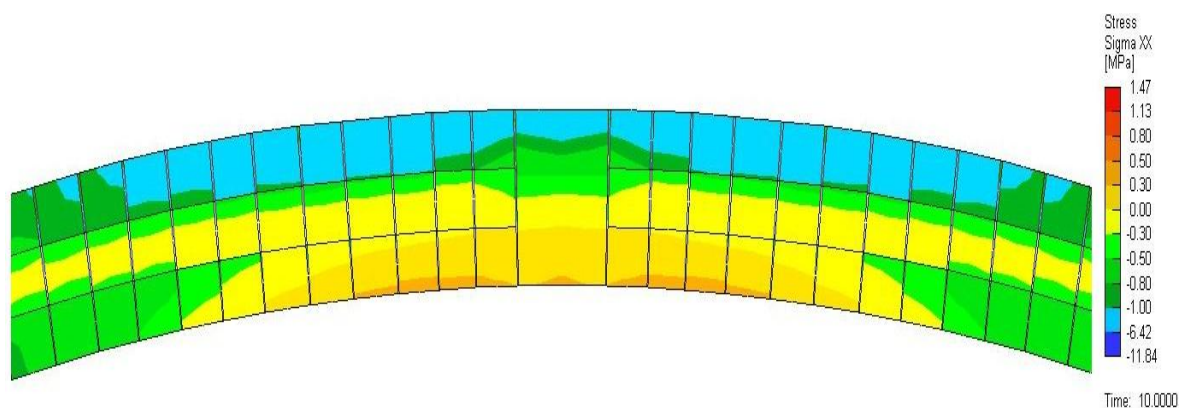


Figure 19: Stress in the longitudinal direction in the vault section - detailed cut-out of the mid-span area - maximum 1.47 MPa, minimum -11.84 MPa. At the interface between yellow and orange the stress value is 0. It can be seen that most of the cross section is still compressed.

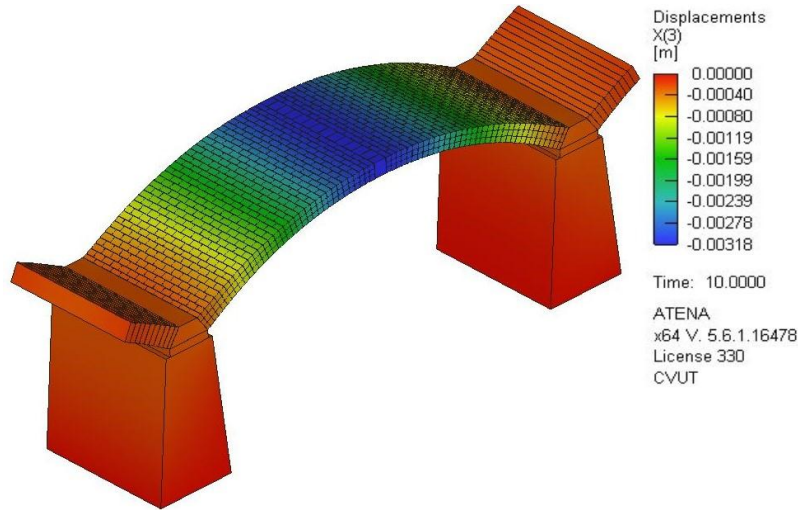


Figure 20: Vertical deformation only for stone vault. The highest deflection is 3.18 mm.

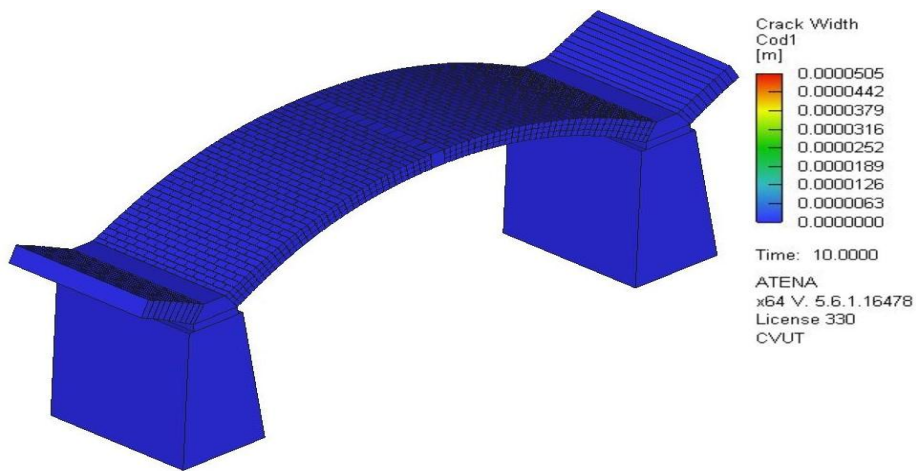


Figure 21: Cracks in the stone vault structure, maximum width 0.05 mm.

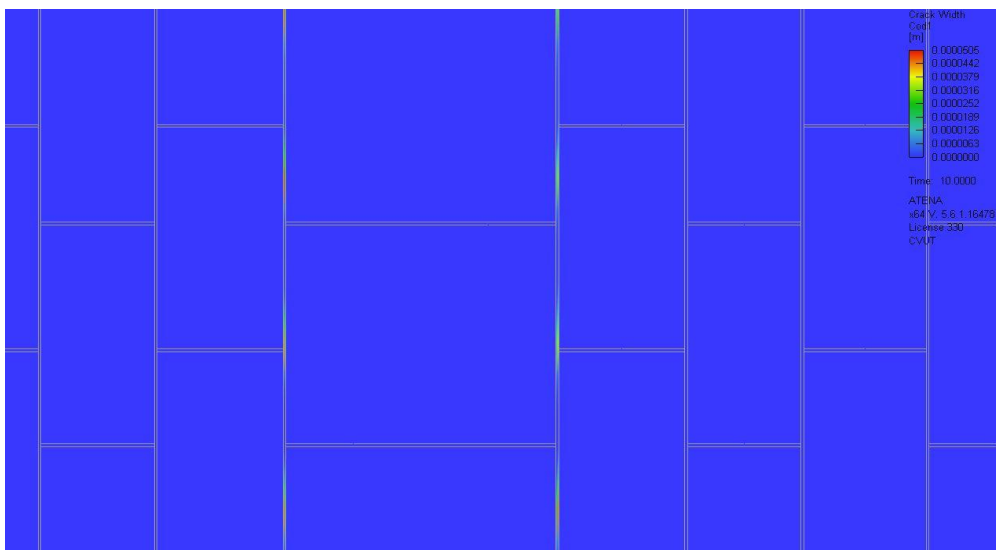
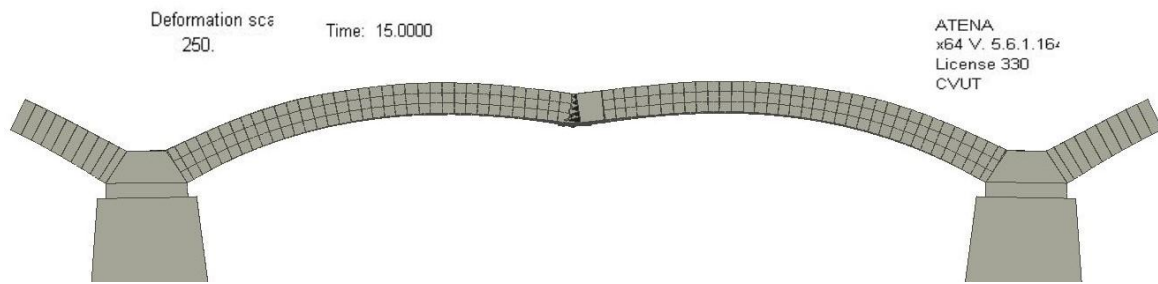


Figure 22. Detailed view of the lower surface of the vault in the middle of the span at the locations of the cracks.



### 4.3 Temperature loading results



**Figure 23: Deformed shape under temperature loading, deformation scale 250:1. There is a clear hinge formation in the centre of the vault span.**

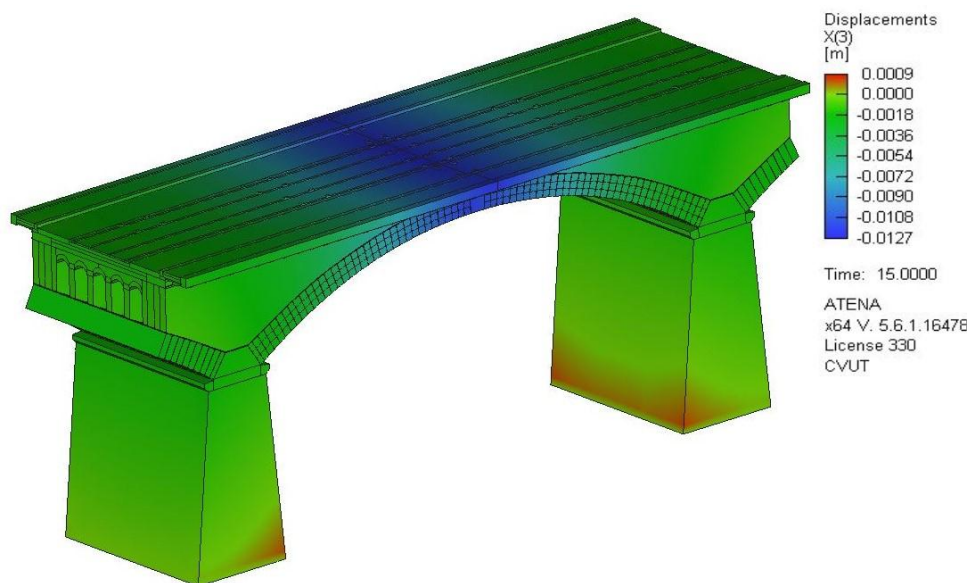


**Figure 24: Vertical deformation - maximum deflection 12.7 mm.**

### 4.4 Summary of results

In general, the results can be summarized by the fact that there is a stretched region at the bottom of the cross-section in the area of the peak of the arc. Cracks of widths of a few hundredths of a mm occur locally in the joints. However, the majority of the cross-section remains compressed. It can therefore be said that the structure behaves as expected for the applied loads and its stability is not compromised. The structure meets the full load capacity conditions for the load combinations considered.

The application of the thermal load (cooling of the structure) caused the formation of a joint in the top of the stone vault. The masonry structure, due to the large number of contact joints between the masonry elements, has a high capacity to release the stresses arising from the thermal loads and in the extreme case it can start to behave as a structure with 1 to 3 hinges.

Therefore, the thermal load has no significant effect on the function of the structure and is therefore not considered in combination with traffic loads.

As part of the analysis, the reinforced concrete bearing structure of the pavements, relief chambers and walls included in the model was also assessed in a simplified form. Based on the results, it can be said that, in the case where the reinforcement of the cantilevers is not weakened by corrosion, these elements are safe to carry pedestrian loads. No excessive stresses were found for the relief chambers and walls.

## 5. CONCLUSION

This numerical analysis was performed to recalculate the load capacity of the existing structure of the arches of the Palacký Bridge and to assess its structural parts.

The results are based on the values of material characteristics obtained during the diagnostic survey. The shape and centrelines of the individual arches were verified both in the original documentation and by the diagnostic survey and an important basis for the analysis.

The following calculations and analyses were performed as part of this report:

- Determination of the load capacity of the vaults.
- Assessment of the relief chambers, headwalls and bridge foundations.

The load capacity of the structure is calculated in combination without thermal loads, which have an insignificant effect on the load capacity of the structure. The masonry structure, due to the large number of contact joints between the masonry elements, has a high capacity to relieve stresses arising from thermal loads and in the extreme case may start to behave as a structure with 1 to 3 hinges. Therefore, the thermal load has no significant effect on the function of the structure and is therefore not considered in combination with traffic loads.

Relief chambers, backfill and reinforced concrete extensions of the bridge have a significant influence on the behaviour of the structure. They help to distribute the applied traffic load and dampen the dynamic phenomena it causes.

The existing condition of the arches of the Palacký Bridge appears to be good and the structural arrangement of the bridge has proved to be functional from a structural point of view.

The chosen procedure for the design of the structure using non-linear analysis has led to relevant results on a model that corresponds in its behaviour to the real structure.

## REFERENCES

1. ČSN EN 772-1+A1 Test methods for masonry elements. Part 1: Determination of compressive strength.
2. ČSN EN 998-2 Specifications of mortars for masonry. Part 2: Mortar for masonry.
3. ČSN EN 13791 - Assessment of in-situ compressive strength in structures and precast concrete component.
4. ČSN 73 0038 - Design and Assessment of Building Structures in Conversions.
5. ČSN EN - Eurocode: Basis of structural design, set of standards, 1990.
6. ČSN EN– Eurocode 1: Actions on structures, set of standards, 1991.
7. ČSN EN- Eurocode 2: Design of concrete structures, set of standards, 1992.
8. ČSN EN - Eurocode 6: Design of masonry structures, set of standards, 1996,
9. ČSN 73 6222 - Load capacity of road bridges.
10. ČSN ISO 13822 - Principles of structural design. Evaluation of existing structures.
11. Červenka, V., Jendele, L. and Červenka, J. Atena program documentation, Part 1 – Theory. Cervenka Consulting, 2018.
12. Červenka, J. and Papanikolaou, V.K. Three dimensional combined fracture-plastic material model for concrete. Int. journal of plasticity, 2008.
13. Červenka, V., Červenka, J. and Pukl, R. ATENA – a tool for engineering analysis of fracture in concrete. Sadhana, 2002.
14. Hill, R. *The Mathematical Theory of Plasticity*. Oxford: Clarendon Press, 1950.